Chemosphere 308 (2022) 136362

Contents lists available at ScienceDirect

Chemosphere

journal homepage: www.elsevier.com/locate/chemosphere

Toxic effects of polystyrene microplastics on the intestine of *Amphioctopus fangsiao* (Mollusca: Cephalopoda): From physiological responses to underlying molecular mechanisms

Jian Zheng [a,b], Congjun Li [c], Xiaodong Zheng [a,b,*]

[a] Institute of Evolution & Marine Biodiversity (IEMB), Ocean University of China, Qingdao, 266003, China
[b] Key Laboratory of Mariculture, Ministry of Education, Ocean University of China, Qingdao, 266003, China
[c] Laboratory of Marine Protozoan Biodiversity and Evolution, Marine College, Shandong University, Weihai, 264209, China

HIGHLIGHTS

- Microplastic exposure caused intestinal toxicity damage of *Amphioctopus fangsiao*. this study, the octopus *A. fangsiao* were exposed to microplastics (polystyrene microplastics, Micro-PS) at concentrations of 100 and 1000 μg/L for 21 days, and then the physiological response, histopathological analysis, biomarkers of oxidative stress and glycolipid metabolism, microbiome perturbations and transcriptomic profiles in the intestines were performed.
- The first assessment of the toxic impact of microplastic on octopus is reported.
- Multiple approaches were used to perform the comprehensive analysis.

GRAPHICAL ABSTRACT

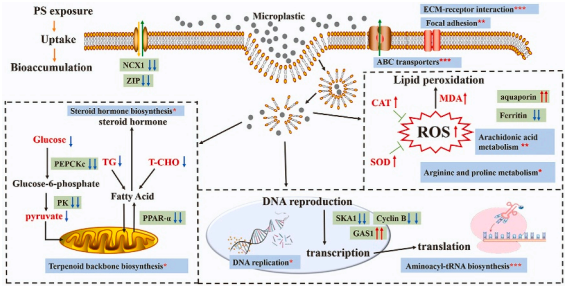

ARTICLE INFO

Handling editor: James Lazorchak

Keywords:
Microplastics
Amphioctopus fangsiao
Toxic effects
Intestine

ABSTRACT

Microplastics are broadly used and among the most studied environmental pollutants due to their potential impacts on organisms and human health. *Amphioctopus fangsiao* (Cephalopoda: Octopodidae) is an important commercial species in the Pacific Northwest and is very popular among consumers owing to its rich nutritional value and fresh flavor. However, the toxic effects of microplastic exposure on *A. fangsiao*, including phenotypical effect and underlying molecular mechanism, remain limited. In this study, the octopus *A. fangsiao* were exposed to microplastics (polystyrene microplastics, Micro-PS) at concentrations of 100 and 1000 μg/L for 21 days, and then the physiological response, histopathological analysis, biomarkers of oxidative stress and glycolipid metabolism, microbiome perturbations and transcriptomic profiles in the intestines were performed. Results demonstrated that Micro-PS exposure had distinct adverse effects on the food intake of *A. fangsiao*. Histological analysis revealed that Micro-PS exposure has resulted in histopathological damage, thus causing early inflammation of the intestine. Oxidative stresses, metabolic disorders and microbiome perturbations were also detected in the intestine of *A. fangsiao* based on physiological biomarkers and microbiome analyses. Moreover, transcriptome analysis detected the differentially expressed genes (DEGs) and significantly enriched KEGG pathways in response to oxidative stress, glycolipid metabolism, DNA damage and transmembrane transport of intestinal

* Corresponding author. Institute of Evolution & Marine Biodiversity (IEMB), Ocean University of China, Qingdao, 266003, China.
E-mail address: xdzheng@ouc.edu.cn (X. Zheng).

https://doi.org/10.1016/j.chemosphere.2022.136362
Received 1 July 2022; Received in revised form 29 August 2022; Accepted 3 September 2022
Available online 7 September 2022

cells, revealing distinct toxic effects at the molecular level. In summary, Micro-PS exposure has a strong impact on the intestines of *A. fangsiao*. For the first time, this study uses multiple approaches based on the physiological and biochemical response as well as transcriptional regulation analysis. The first assessment of the toxic impact of this species under Micro-PS exposure is also reported.

1. Introduction

Microplastics, synthetic polymers of 1 μm–5 mm in size, have been found in a diverse range of marine organisms (Lusher, 2015; Nelms et al., 2018; Kuhn and van Franeker, 2020). The ultimate sink of microplastics is in the seafloor where its accumulation rates and composition have been influenced by the interaction between human activities and the natural environment (Pham et al., 2014). It is reported that at least 35,500 metric tons of microplastics were detected on the ocean surface in 2014 (Eriksen et al., 2014), and the densities of 10 and 100 μm in size ranged from 0.029 to 2.9 μg/L (Beiras and Schönemann, 2020). Besides, large amounts of microplastics have also been found on the city coastline (Thiel et al., 2013; Garces-Ordonez et al., 2020; Zuo et al., 2020). For example, previous studies have detected high abundances of microplastics with 0.02–5 mm in size along the coast of south China (3300–990,000 items m^{-2}) (Dou et al., 2021), and this amount on the coast near South Korea was 1400–65000 items m^{-2} (Eo et al., 2018). Due to high densities, debris on shores close to cities can exert a huge influence on benthic habitats where faunae are very sensitive to environmental pollution (Galgani et al., 2015; Angiolillo and Fortibuoni, 2020). The interactions between microplastics and marine organisms include the damage of microplastic exposure to marine organisms and the adaptations of these organisms to microplastic pollution (Kühn et al., 2015; Consoli et al., 2019; Angiolillo et al., 2021; Pedà et al., 2022). There are many types of microplastics distributed in the ocean, of which polystyrene (Micro-PS) is one of the most common and abundant found in the marine environment (Qiao et al., 2019). Many studies have proved the adverse effects of Micro-PS exposure on morphology, reproduction, physiological behavior, oxidative stress, energy and lipid metabolism, intestinal microbiome community, and gene expression of marine organisms (Green, 2016; Sussarellu et al., 2016; Qiao et al., 2019; Hirt and Body-Malapel, 2020; Teng et al., 2021; Ory et al., 2018).

As a widely exploited marine resource around the world, cephalopods, especially octopuses, have a relatively short life expectancy, resulting in high growth rates and metabolic rates (Zielinski and Pörtner, 2000). The characteristics of small-scale activity areas and territorial nature allow they can indicate the quality of the coastal habitat environments (Arechavala-Lopez et al., 2018; Sillero-Ríos et al., 2018). Moreover, as generalist predators, octopuses are more likely to accumulate pollutants in their bodies, such as microplastics and heavy metals, both from the prey and the environment (Mangold, 1983; Bo et al., 2020; García et al., 2002; Jiang et al., 2020b). They thus have been proven as a potential indicator organism of environmental pollution (Raimundo et al., 2010; Semedo et al., 2014; Sillero-Ríos et al., 2018). A recent study reports the microplastic composition including polymer type, color and shape in two cephalopods (*Vampyroteuthis infernalis* and *Abralia veranyi*) with different ecological behaviors, which explained the great biological effect of microplastic sinking mechanism on cephalopods (Ferreira et al., 2022). And the microplastics presence in *Octopus vulgaris*, *Sepia officinalis* and *Dosidicus gigas* were also detected in many studies (Oliveira et al., 2020; Gong et al., 2021; Pedà et al., 2022). However, the damages of microplastic exposure to cephalopods, including the physiological response and molecular mechanism, are still unexplored. It is necessary to better understand the potential impact of microplastics on cephalopods using synthetical studying methods. As an important economic species of cephalopods, Octopus *Amphioctopus fangsiao* is not only widely distributed in the northwest Pacific Ocean, but also a potentially suitable species for industrial aquaculture (Jiang et al., 2020b). Lately, many studies have focused on fishing, farming and classification of *A. fangsiao* (Jiang et al., 2020a; Tang et al., 2021; Bao et al., 2022). The characteristics of clear life history and easy accessibility of this species make it suitable for toxicological studies (Jiang et al., 2020a).

The intestine is one of the organs with the highest accumulation of microplastics (Bidder, 1966; Lipiński, 1990; Hirt and Body-Malapel, 2020). Many recent studies have demonstrated the possible adverse effects of microplastic exposure on intestinal microbiota, intestinal homeostasis and immune response (Qiao et al., 2019; Hirt and Body-Malapel, 2020; Jin et al., 2018). In this study, we conducted the measurement of food intake, histopathological damage and physiological biomarkers, transcriptome sequencing and microbiome analysis for *A. fangsiao*, a marine benthic cephalopod, grown under exposure to microplastic. Our data provide a comprehensive insight into the mechanism of interaction between microplastic and octopus intestine. This work also demonstrates the power of combining physiological response, transcriptome and microbiome analysis in gaining a panoramic view of protist responses to microplastic stress.

2. Materials and methods

2.1. The preparation of Micro-PS and experimental animals

The 5 μm-size Micro-PS has been found to accumulate more in the intestines based on previous studies (Qiao et al., 2019). Thus, the Micro-PS (diameter: 5 μm) was selected in this study, purchased from Tianjin BaseLine ChromTech Research Centre. The stock suspension of Micro-PS was first prepared using 0.00001% v/v Tween-20 as surfactant to avoid Micro-PS sticking to the tank walls or clumping together. Tween-20 with low concentration has few toxicities for marine invertebrates as described by Sussarellu et al. (2016). A total of 5 g Micro-PS was added to 500 ml Milli-Q water, and the suspension was sonicated. The Micro-PS particles suspended on the surface were removed, and the remaining uniformly distributed Micro-PS suspension is stored at 4 °C.

The concentration of Micro-PS in the suspension was calculated by evaporating the water and weighing the remaining particles. Firstly, the suspension with a certain volume was poured into the weighed Petri dish. This Petri dish was put into the oven at 56 °C for 12 h to evaporate the water. It was then weighed. The equation for calculating the concentration of Micro-PS according is as follows:

$$C = (W_1 - W_0)/V$$

where C is the concentration of Micro-PS (g/L) (the concentrations were averaged in triplicate), W_0 is the weight of the Petri dish (g), and W_1 is the weight of the Micro-PS and Petri dish after evaporation (g). V is the volume poured into the Petri dish.

The suspension with determined concentration was diluted into 100 μg/L and 1000 μg/L for exposure experiment.

A total of 54 adult *A. fangsiao* (≈200 days post-hatch) individuals, with an initial mantle length of 65.15 ± 13.35 mm and weight of 57.145 ± 21.839 g, were collected from a private enterprise (Jiaxin Aquaculture Farm, China). All individuals were housed in an environmentally controlled setting (temperature: 17–18 °C, pH: 7.9–8.2, salinity: 32, dissolved oxygen: > 6.5 mg/L, 14:10 h light: dark cycle) for one week to acclimatize. Then, they were placed in eighteen 90-L glass tanks (60cm × 50cm × 30 cm, three octopuses per tank). Then the ceramic shelters were placed around each octopus to avoid fighting. Octopuses were overfed with living clam (*Ruditapes philippinarum*) (15–16 clam

individuals in each tank, collected from Jiaxin Aquaculture Farm) every day. The continuous aeration was carried out throughout the study.

2.2. Experimental exposure of octopuses to Micro-PS

The eighteen experimental tanks were randomized into three groups: Control group (Control, 0 μg/L), low-concentration of Micro-PS group (PS-L, 100 μg/L) (close to the microplastics concentration at the seabed) and high-concentration of Micro-PS group (PS–H, 1000 μg/L) (a concentration that can trigger more physiological and molecular responses of octopus). The Micro-PS per treatment were diluted from stock solutions. During experimental exposures, half of the seawater was renewed daily in all tanks, and the corresponding Micro-PS solution was added to achieve the target concentrations in each treatment. The seawater with Micro-PS in different concentrations was renewed every day. To keep Micro-PS relatively evenly distributed, the aeration intensity and the positions of the air stone in all tanks were changed twice a day. During the 21-day exposure experiment, all other farming conditions were consistent among the three groups.

2.3. Food intake and specific growth rate calculation

To analyze the effect of Micro-PS exposure on physiological behavior, one octopus in each tank was separated by a glass partition and fed separately during experimental exposures to measure food intake on day 0, day 7, day 14 and day 21. The octopuses were fed with enough clams every day after being weighed, and food debris was cleaned up and weighed at the same time the next day. The equation for calculating food intake according to Song et al. (2020) is as follows:

$$FI = W_{S1} - W_{S2}$$

where the FI is food intake (g), W_{S1} is the weight of the feed (g), and W_{S2} is the weight of food debris on the following day (g).

The initial body weight and the final body weight at the end of the rearing period were measured (precision 0.01 g). The growth performance of *A. fangsiao* in three groups was calculated using the following formulas:

$$\text{Specific growth rate (SGR, \%)} = [\ln(\text{final body weight}) - \ln(\text{initial body weight})]/\text{exposure time}.$$

The GraphPad Prism 9.0 software was used to conduct the statistical analysis. The obtained data were statistically analyzed using a paired sample *t*-test, with a difference of $p < 0.05$ being considered significant. The mean ± standard deviation (S.D.) was used to express all the data.

2.4. Histological analysis

After 21-days of exposure, 15 octopuses (5 individuals per group) were randomly selected to measure the damage of Micro-PS exposure. The intestinal tissues were fixed in Bouin's fixative for 24 h. The tissues were embedded in paraffin wax, sectioned at 5 μm-thickness and mounted on slides on the following day. Each slide was then deparaffinized and rehydrated by xylene and graded alcohol series, respectively. After staining in the hematoxylin-eosin (HE), the slides of each sample were observed using optical microscope.

2.5. Physiological biomarker analyses and integrated biomarker response (IBR) analysis

After 21-days of exposure, for the determination of biomarkers, the intestinal tissues (10 g) from 6 freshly killed octopus per group were homogenized in 5 ml of 50 mM PBS (pH7.5) containing the protease inhibitors. The homogenates were centrifuged at 6000 *g* at 4 °C for 15 min, and then the supernatants were collected. The protein concentrations of tissue extracts were determined with BCA Protein Assay Kit (Biotime, China). According to the methods described by previous studies (Spitz and Oberley, 1989; Okutan et al., 2005; Hsu et al., 2008; Dong et al., 2013), the measured total protein level was used for detecting the oxidative stress parameters and enzyme activity by commercial kits (Biotime, China), including ROS content, lipid peroxidation's level (malondialdehyde (MDA), a metabolite of lipid peroxidation), and activities of superoxide dismutase (SOD) and catalase (CAT). In addition, the analyses of glycolipid metabolism responses (Glucose, Glu; Pyruvic acid, Pyr; Total cholesterol, T-CHO; Triglyceride, TG) were performed using the commercial kits from Nanjing Jiancheng Bioengineering Institute (Nanjing, China) as described by Teng et al. (2021). Similarly, the paired sample *t*-test was used to conduct the statistical analysis.

IBR, a multi-biomarker approach for assessment of the potential impacts of environmental stress on organisms, was used in this study. This method integrated biomarker responses into a stress index (IBR). According to Sanchez et al. (2013), the index "Integrated Biological Responses version 2" modified from the version described by Beliaeff and Burgeot (2002) was applied to evaluate the combined effects of Micro-PS on *A. fangsiao*.

2.6. Intestinal microbiome analysis

The intestinal tissues of 12 octopuses after 21-day exposure experiment (6 individuals from the Control group and 6 individuals from PS-H group) were used to perform microbiome analysis. The total genomic DNA of intestinal tissues was extracted using FastDNA Soil Kit (MP Biomedicals, USA). The samples, satisfying the requirement by Nanodrop and Qubit detection, were used to amplify the V3+V4 region of 16 S rDNA in bacteria. The process of library construction is as follows: the primers were designed based on the conserved region of V3+V4 region and added sequencing adapters in the end of these primers; The target sequences were amplified, purified and homogenized. These sequences were composed of a sequencing library. All qualified libraries were then sequenced using Illumina Novaseq 6000. The raw reads obtained by sequencing were stored in FASTQ format file and filtered to generate clean reads by Trimmomatic v0.33 (Bolger et al., 2014) and Cutadapt 1.9.1 (Martin, 2011). UCHIME v4.2 was used to identify and remove the chimeric sequences, generating effective reads (Robert et al., 2011).

The operational taxonomic unit (OTU) was generated by Usearch (Edgar, 2013). Venn diagram was generated to visualize the common and unique features among samples (Hanbo and Paul, 2011). SILVA was used as a reference database for taxonomic annotation of feature sequences. The composition of bacteria in each sample was calculated at the level of phylum and genus. The abundance of each species and the distribution histogram at phylum and genus taxonomic levels were generated by QIIME (Caporaso et al., 2010). Unweighted Pair-group Method (UPGMA) was used to construct clustering tree that reflected similarities between samples (Hua et al., 2017). The histogram of species composition combined with UPGMA clustering tree was constructed to show the similarity in the abundance of bacteria and the similarity between samples. All samples were classified to show the difference in species diversity based on Principal coordinates analysis (PCoA) (Gower, 1966). The test of significant difference was performed in beta diversity between groups based on PERMANOVA analysis using vegan

pack in R language (Anderson, 2005). Rank abundance curve was generated to show the richness and evenness of species composition (Kõljalg et al., 2013).

2.7. Transcriptome analysis

Total RNAs of the intestinal tissues from 6 octopuses after 21-day exposure experiment (3 individuals from Control group and 3 individuals from PS-H group, duplicate individuals with microbiome analysis) were isolated by commercial kits Total RNA extraction kit (Omega). The integrity, concentration and purity were detected by NanoDrop 2000) (Thermo). The samples satisfying the requirement were used for library construction. The process of library construction is as follows: the magnetic beads with Oligo(dT) were used to isolate mRNA; Enriched mRNA was randomly fragmented by Fragmentation Buffer; Fragmented mRNA was then used as the template to purify the cDNA; Double-strand cDNA was amplified by PCR to obtain cDNA library. The qualified library examined by Qubit 2.0 and Agilent 2100 was sequenced on the Illumina sequencing platform.

Raw data containing useless data was filtered by trimming adapter contaminations and removing nucleotides with low Quality-score. Filtered clean data was stored in FASTQ format file. The clean reads were mapped to the reference genome sequence of *A. fangsiao* (unpublished data) using HISAT2 (Kim et al., 2015). The mapped reads were assembled and quantified by StringTie (Pertea et al., 2015). HMMER3, BLAST2GO, KOBAS and DIAMOND were used to annotate gene functions based on NCBI non-redundant protein sequences (Nr), Gene Ontology (Go) and Kyoto Encyclopaedia of Genes and Genomes database (KEGG).

The differential expression genes (DEGs) between groups were detected using DEseq2. The filtering thresholds were set to q-value (Adjusted p-value) ≤ 0.05 and the $|\log_2(\text{fold change})| \geq 1$ (Love et al., 2014). These DEGs were then classified by GO terms and KEGG pathways. The phyper function in R software was used for enrichment analysis. The GO terms and KEGG pathways with p-value ≤ 0.05 were used as significant enrichment.

2.8. RT-qPCR verification

According to the results of GO and KEGG enrichment analysis, ten DEGs involved in oxidative stress, antioxidant enzyme, glucolipid metabolism and DNA damage were selected for qRT-PCR analysis to validate the sequencing data. *β-actin* gene and *GAPDH* gene were selected as the internal standardization reference. The primer sequences designed to amplify reference genes and DEGs were shown in Table S1. LightCycler Roche480 was used to perform qRT-PCR. The reaction system was 20 μL containing 2 μL cDNA template, 0.4 μL of primers and ROX Reference Dye (50x), 10 μL of TB Green® Premix Ex TaqTM (2x) and 6.8 μL of RNase-free water. The amplification conditions as follows: 15 s denaturation (95 °C), 40 alternating cycles of 5 s (95 °C), denaturation 15 s (60 °C) and 35 s (72 °C). To reduce technical error, triplicates on each sample were performed. The relative expression was calculated by the comparative cycle threshold ($2^{-\Delta\Delta Ct}$) method.

3. Result

3.1. Micro-PS exposure restrained the food intake

No significant differences in food intake were observed in all three groups after 7 days and 14 days of exposure. Of note, after 21-days exposure, addition of high-concentration of Micro-PS was able to considerably reduce the food intake of *A. fangsiao* ($p < 0.05$). In the control group, there was little difference in food intake of octopus at different exposure time stages. The food intake in the PS-L group showed an increasing trend after a relative decrease, while the PS-H group had gradual reductions in food intake (Fig. 1). The SGR of *A. fangsiao* in three

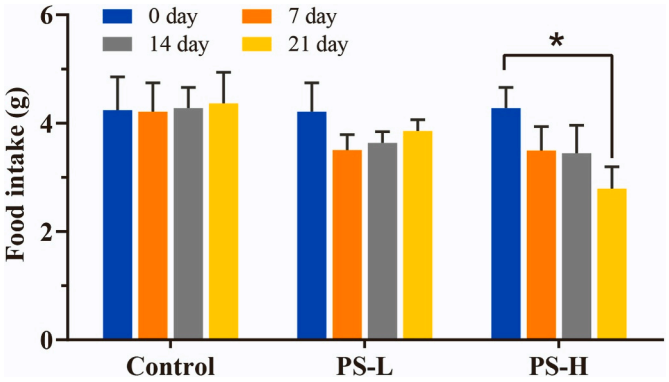

Fig. 1. Food intake in different treatments. Data represent mean ± S. D. (n = 6). *$p < 0.05$.

treatment groups was 1.094 ± 0.032%, 0.956 ± 0.083% and 0.823 ± 0.186%, respectively. High-concentration of Micro-PS has significantly reduced the growth performance of *A. fangsiao*.

3.2. Micro-PS exposure caused histological damage to the intestine

The paraffin section was used to explore the damage to the intestine treated with Micro-PS. As shown in Fig. 2A and D, the lamellae of intestine with well-defined were observed in the control group. However, there was significant histopathological damage in PS-L (Fig. 2B and E) and PS-H groups (Fig. 2C and F) after 21-days exposure, that is, the shedding of microvilli, the increase of vacuolization and goblet cell, cytoplasmic damage dispersion and the looseness of connective tissue. This indicated that Micro-PS exposure has caused distinct histopathological changes in the intestine of octopus.

3.3. Micro-PS exposure induced oxidative stress and the glucolipid metabolism disorders

Fig. 3A showed the changes in ROS levels. Compared with the control group (3.02 ± 0.013 fluorescence intensity/mg protein), the mean values of ROS content in the PS-L and PS-H groups have remarkably increased (4.19 ± 0.069 and 4.31 ± 0.050 fluorescence intensity/mg protein, $p < 0.001$) (Table S2), indicating that Micro-PS exposure induced the rising of ROS level in the intestines. The content of MDA in control group was 2.59 ± 0.066 μM/mg protein, while the values in the PS-L and PS-H groups were 2.53 ± 0.092 and 2.20 ± 0.165 μM/mg protein (Fig. 3B, Table S2). It was clear that the level of lipid peroxidation increased significantly in the high-concentration of Micro-PS treatment ($p < 0.05$). Similarly, as shown in Fig. 3C and D, the mean values of SOD (11.80 ± 0.550 and 13.75 ± 0.51 U/mg protein) and CAT (11.03 ± 0.650 and 13.12 ± 0.61 μM/min/mg protein) activities in the intestines of the PS-L and PS-H treated octopuses were markedly increased, compared with the control group (9.34 ± 0.087 μmol/mg protein) ($p < 0.05$; $p < 0.01$; $p < 0.001$) (Table S2). These indicated that the level of oxidative stress parameters including ROS and MDA were all significantly increased under Micro-PS exposure stress, leading to the imbalance of homeostasis. And the antioxidant enzyme activities of SOD and CAT were stimulated due to the oxidative damage caused by Micro-PS stress.

To explore the variation of glucose metabolism and lipid metabolism, Glu, Pyr, T-CHO and TG levels in intestinal tissue of *A. fangsiao* were detected after Micro-PS exposure (Fig. 3E-H). Glu and Pyr, which play a crucial role in glycolysis, have considerably decreased in the Micro-PS exposure groups (Fig. 3E and F). Similarly, the T-CHO and TG involved in lipid metabolism showed a similar decline trend (Fig. 3G and H). These data clearly suggested that exposure to Micro-PS significantly disturbed the glucolipid metabolism.

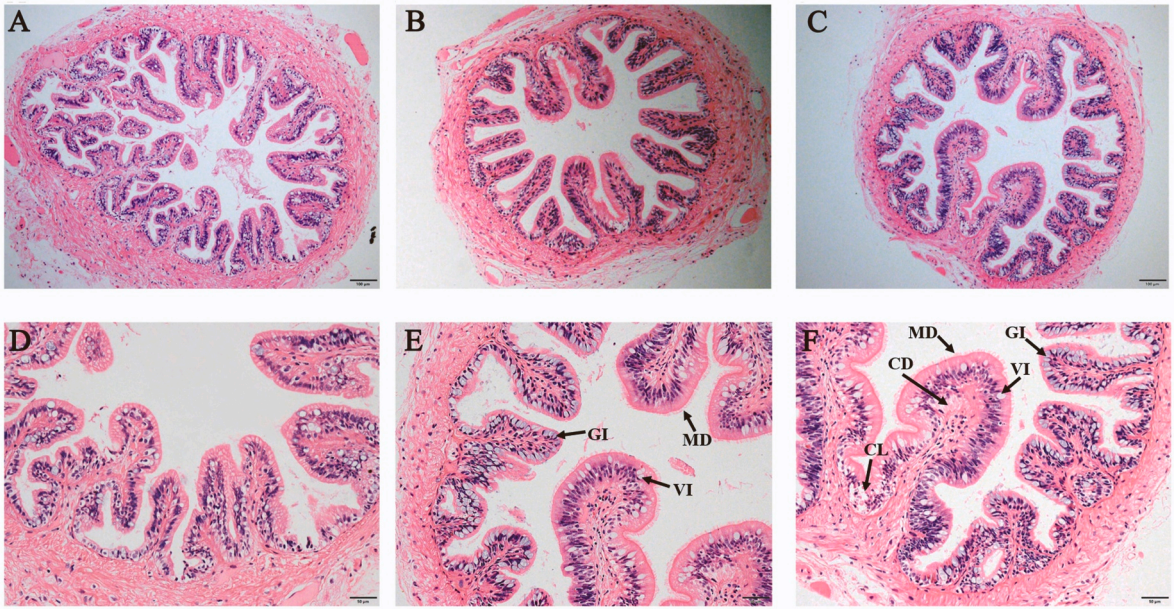

Fig. 2. Micrographs of intestine in control group (**A** and **D**), PS-L group (**B** and **E**) and PS-H group (**C** and **F**) after 21-days exposure to Micro-PS. The scale bar of the A-C and D-E was 100 μm and 50 μm, respectively. GI: goblet cell increase, VI: the increase of vacuolization, MD: The shedding of microvilli, CD: cytoplasmic damage dispersion, CL: the looseness of connective tissue. The sections are of 5 mm thickness, stained with hematoxylin and eosin.

3.4. Integrated biomarker response

The integrated biomarker response (IBR) index integrated multiple datasets from the above biochemical parameters and biomarkers was calculated to show a comprehensive description of the health status of *A. fangsiao* under environmental stress. It can be used to assess the integrated response of biomarkers in tissues (Samanta et al., 2018). High IBR values generally indicate increased toxic stress in tested organisms (Teng et al., 2021). Oxidative stress parameters (ROS, MDA), antioxidant enzyme (SOD, CAT) and glucolipid metabolism biomarker (Glu, Pyr, T-CHO, TG) responses in different treatment groups are presented in star plots (Fig. 3I). The degree of stress in each treatment group can be evaluated according to calculated IBR values. In this study, the IBR index increased with concentration-dependent after 21-days exposure (Fig. 3J).

3.5. Micro-PS exposure induced microbiome perturbations

Microbiome analysis between control and PS-H groups was carried out based on high-throughput sequencing to assess the damages to the intestinal microbiome community of *A. fangsiao* under Micro-PS exposure. A total of 840 OUTs were obtained from all samples, of which 746 OTUs were shared by the control and PS-H groups, 74 OTUs and 20 OTUs were separately distributed in the control and PS-H group, respectively (Fig. 4A). PCoA analysis presented the principal coordinate analysis plot of bacteria, which showed that two groups were accurately separated by the first two principal components. The contribution rate of PCoA1 and PCoA2 to explain the variation of bacterial community composition were 62.75% and 22.75%, respectively (Fig. 4B). The contribution rate of PCoA1 was higher than 50%, demonstrating that the differences in bacterial community composition among the samples could be mainly evaluated by the distance on the PCoA1 direction. As shown in Fig. 4C, the bacterial ANOSIM analysis plot showed intra-group and inter-group differences. Rank abundance curve was generated by ranking the features in each sample based on abundance (Fig. 4D). The X-axis showed the abundance rank and the Y-axis represented the relative abundance of all samples. The results indicated that the bacterial richness and the species evenness in the control group were significantly greater than those in the PS-H group.

The microbial community structures at phylum and genus taxonomic levels were detected in this study (Fig. 5A). The results revealed that two groups were successfully separated by the UPGMA clustering tree. The major bacterial phyla in the intestines of *A. fangsiao* were Tenericute, Proteobacteria, Spirochaetes and Firmicutes. The relative abundance of Tenericute in PS-H group has remarkably improved compared with the control group, while there was a significantly reduced in the relative abundance of Firmicutes.

To further assess the impact of Micro-PS exposure on microbial community structures, the top 20 abundant genera were chosen for comparative analysis between groups (Fig. 5B). The richness of Lachnospiraceae NK4A136 group, Bacteroides, Lactobacillus, Lactococcus, Lactobacillus and Streptococcus was higher in the control group, while exposure to Micro-PS increased the richness of Mycoplasma.

3.6. Micro-PS exposure induced the transcriptomic responses

The comparative transcriptome analysis between the control group and PS-H group was performed to evaluate the transcriptomic responses of intestinal tissue under Micro-PS stress. A total of 39.38G clean data were generated after filtering. The mapping rate of the clean reads in each sample mapped to the genome of *A. fangsiao* was above 88%, revealing high sequencing quality. Four-major SNP types detected in comparative transcriptome analysis were A-G, G-A, C-T and T-C.

All transcripts were used to perform the principal component analysis (Fig. 6A). The biological replicates of each group were far from the other groups and close to each other. This result revealed the reliability and reproducibility of transcriptomic data. The expressions of DEGs were quantified and analyzed to elucidate the gene expression pattern under environmental stress. A total of 4870 DEGs (2237 up- and 2633 down-regulated) were obtained between groups (Fig. 6C). The heatmap was also constructed to show the expression of DEGs in all samples (Fig. 6B).

The GO enrichment analysis was carried on to explore the function of related differentially expressed genes. The results indicated that the cellular process (GO:0009987), metabolic process (GO:0008152), membrane (GO:0016020), and transporter activity (GO:0005215) were significantly enriched in the PS-H treatment (Supplemental Fig. S1).

The enrichment analysis of KEGG pathway indicated that these DEGs

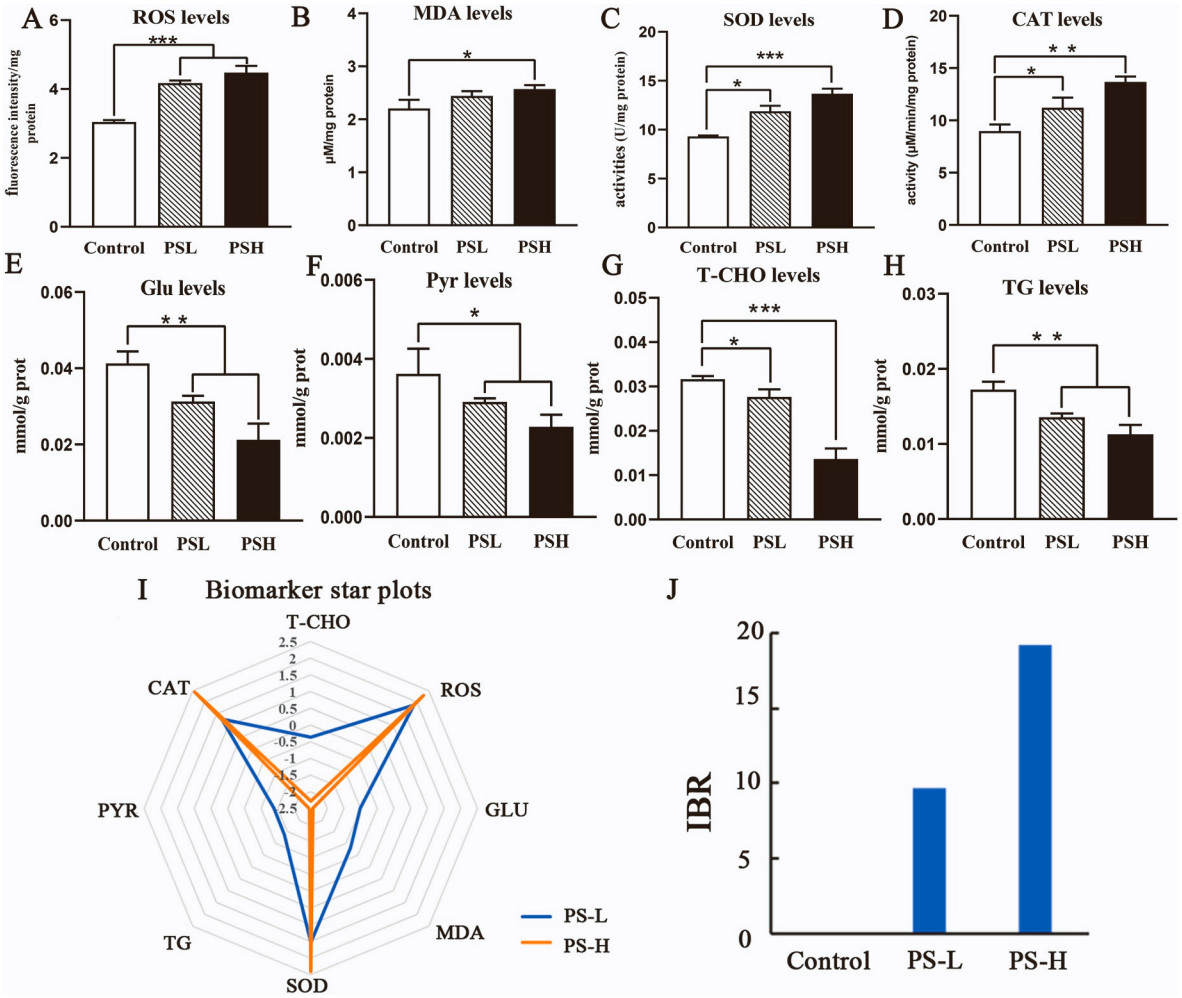

Fig. 3. A-B. the level of ROS and lipid peroxidation in different groups after 21-days Micro-PS exposure, **C-D.** the changes in enzyme activities of SOD and CAT in different groups after 21-days Micro-PS exposure, **E-H.** the changes in glucolipid metabolism responses in the intestines of *A. fangsiao* in different groups after 21-days Micro-PS exposure. Data represent mean ± S. D. (n = 3). $^{***}p < 0.001$, $^{**}p < 0.01$, $^{*}p < 0.05$. **I.** Biomarker star plots in the intestines of *A. fangsiao* after MPs exposure for 21 days. **J.** Calculated IBR index using the biochemical parameters after exposure to Micro-PS for 21 days.

are involved in various pathways. The top 20 pathways were shown in Fig. 7. These pathways mainly involved environmental information processing (ECM-receptor interaction), genetic information processing (aminoacyl-tRNA biosynthesis, ABC transporters), metabolism (retinol metabolism, glycosaminoglycan biosynthesis-chondroitin sulfate/dermatan sulfate), organismal systems (vitamin digestion and absorption), and cellular processes (focal adhesion).

3.7. Validation of DEGs

Ten DEGs involved in oxidative stress, antioxidant enzyme, glucolipid metabolism and DNA damage were selected for qRT-PCR experiment. The melting-curve analysis showed that a single product was amplified for all the tested genes (Fig. S2), indicating that the transcriptome assembly was largely accurate. The results of qRT-PCR revealed consistent expression patterns with transcriptome analysis, confirming that the results of comparative transcriptome analysis were accurate and reliable (Fig. S3).

4. Discussion

This study demonstrates the toxic effects of Micro-PS exposed to *A. fangsiao* based on physiological responses, histological damage, microbiome perturbations and transcriptomic responses. The exposure concentrations of Micro-PS were 100 μg/L (PS-L group) and 1000 μg/L (PS–H group), which were higher than those in the surface waters (Beiras and Schönemann, 2020). Those higher concentrations were selected for the following reasons. Firstly, *A. fangsiao* inhabits the bottom of the sea where the concentration of Micro-PS is high than that in surface water because microplastics tend to clump and stick to the sediment. Secondly, *A. fangsiao* exposed to a high Micro-PS concentration can trigger a fast molecular response, which makes it easier to analyze the toxicological effects and adaptive mechanism. Last but not least, larger toxic effects in *A. fangsiao* caused by high concentration can draw more attention to marine environmental protection and provide a reference for future research.

The results of this study showed that: 1) High concentration of Micro-PS exposure has significantly reduced the food intake and growth performance of *A. fangsiao*. 2) Micro-PS exposure has caused intestinal microbiota disorder and distinct histopathological changes of *A. fangsiao*. 3) Micro-PS exposure has induced oxidative stress and disturbed glucolipid metabolism, and related DEGs and significantly enriched KEGG pathways have also been detected by transcriptome analysis. 4) Micro-PS exposure has altered the transcriptomic profiles, including transmembrane transport of intestinal cells and DNA damage.

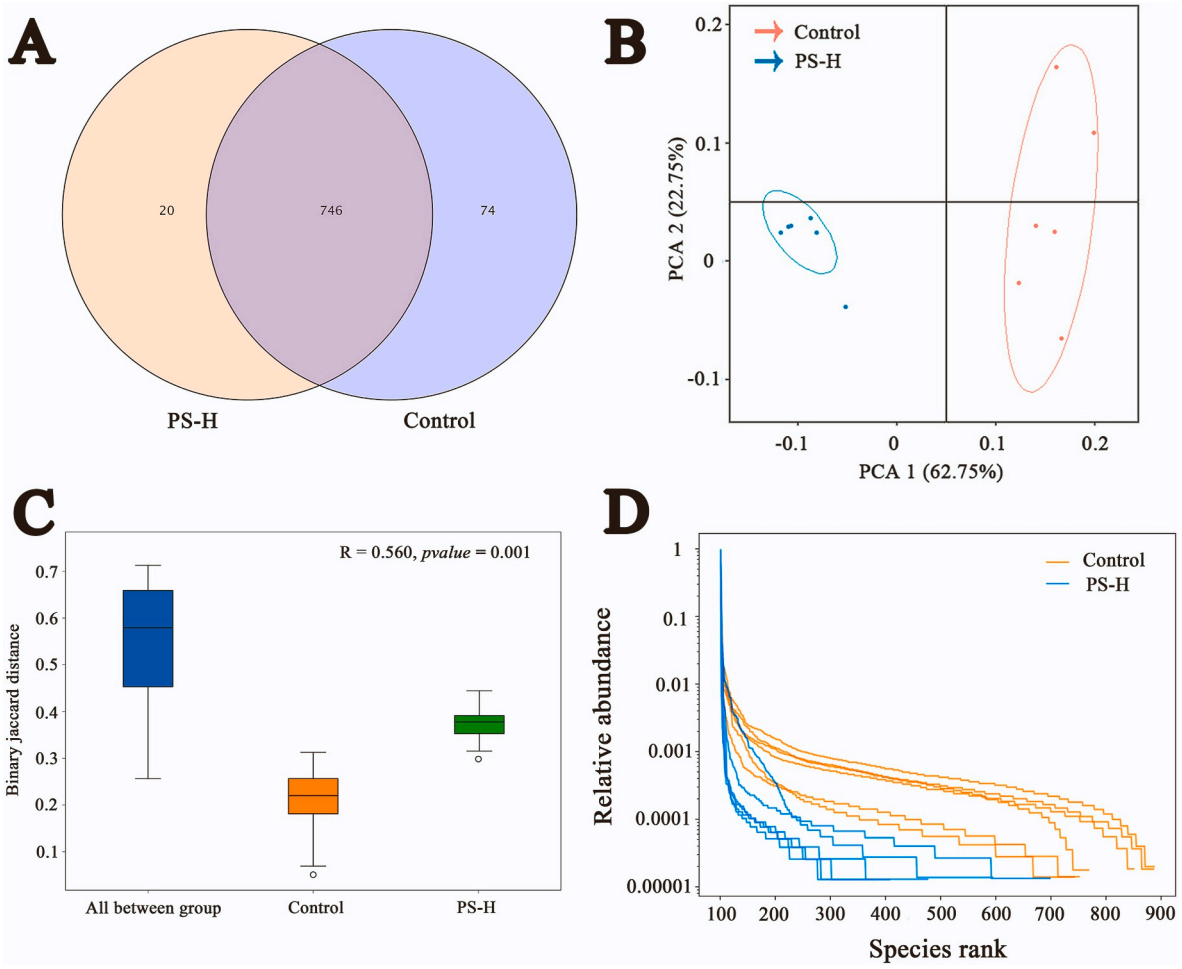

Fig. 4. Intestinal microbiome alterations of *A. fangsiao* induced by 21-days Micro-PS exposure (n = 6). **A.** Venn diagram representing the number of OTUs obtained from control and PS-H groups. **B.** PCA analysis of intestinal microbiome between control and PS-H groups. **C.** ANOSIM analysis plots of intestinal microbiome between the control and PS-H groups. **D.** Rank abundance curve of intestinal microbiome between the control and PS-H groups.

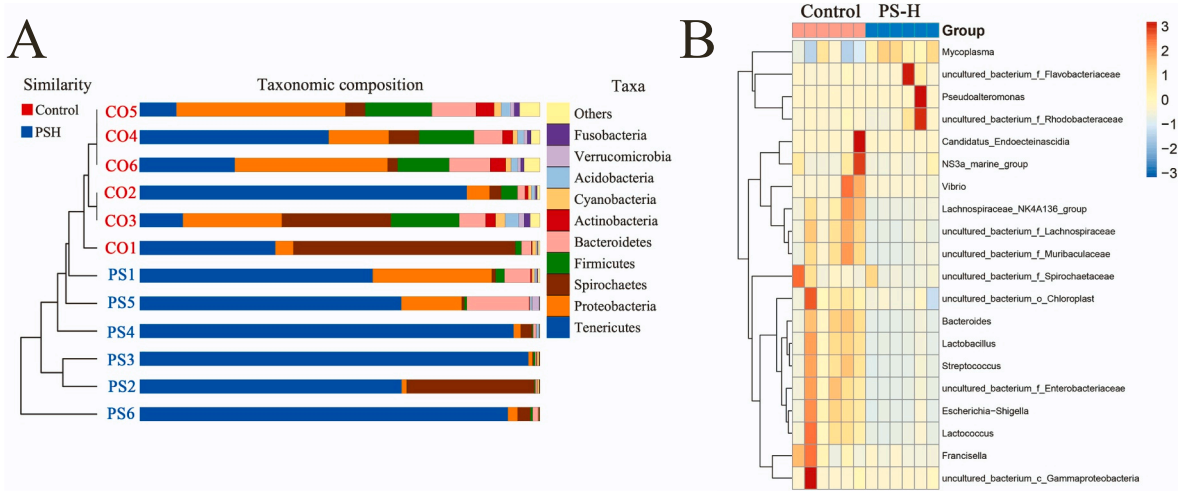

Fig. 5. Composition of intestinal bacterial community of *A. fangsiao* at phylum (**A**) and genus (**B**) taxonomic levels. Only the top 10 most abundant (based on relative abundance) bacterial phyla at the phylum taxonomic level and the top 20 bacterial phyla at the genus taxonomic level were shown.

4.1. Food intake and histological damage

A significant decrease in food intake was detected in PS-H group after 21-days of exposure, which may be an adaptive strategy for *A. fangsiao* to reduce microplastic intake. Similar results were found in the other marine organism, such as *Myitilus edulis*, *Atactodea striata* and *Dreissena polymorpha* (Wegner et al., 2012; Xu et al., 2017; Weber et al., 2020). Many studies have revealed the presence of microplastics in the

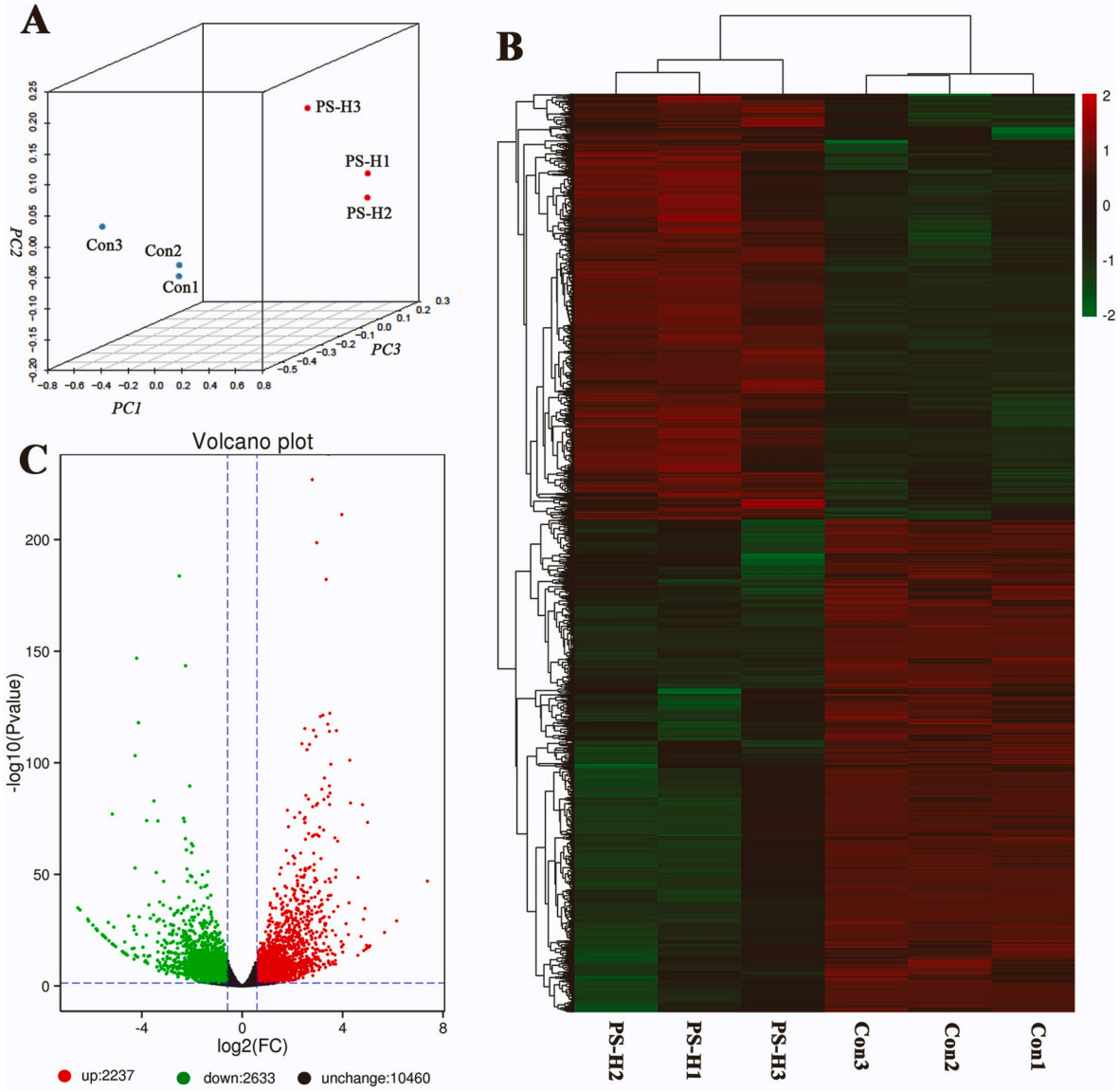

Fig. 6. Characterization of the transcriptome dataset of *A. fangsiao* after 21-days Micro-PS exposure. **A.** PCA analysis shows clear distinctions between control and PS-H groups. **B.** Heatmap showing the altered genes between control and PS-H groups. **C.** Volcanomap shows the number of differentially expressed genes in the intestines (q-value ≤ 0.05).

digestive gland and intestinal contents of benthic and pelagic species (Sanchez et al., 2014; Avio et al., 2015a; Biginagwa et al., 2016). The accumulation of microplastics in the digestive tract and intestine makes digestion increasingly inefficient, leading to a reduction in food intake of *A. fangsiao*. Interestingly, there was an increasing trend after relatively a decline in food intake in the PS-L group. The reason may be the evolutionary adaptation of *A. fangsiao* to the microplastics of low concentrations (Weber et., 2020). The growth performance of *A. fangsiao* under Micro-PS exposure has been significantly low. This result indicated that the growth and energy conversion of *A. fangsiao* have been limited after PS exposure. Microplastic ingestion induced the malabsorption of *A. fangsiao*, and the food intake and conversion were thus decreased. A similar result was also found in other marine organisms (Lucia et al., 2010; Liu et al., 2019; Huang et al., 2021).

Microplastics are taken up into the aquatic organisms via endocytosis and filtered out by the gill. They are transferred via ciliary movement into the mouth, digestive gland and intestines (Wang et al., 2021). Distinct histological damage was found in the intestinal tissue of *A. fangsiao* under Micro-PS stress. Many studies have demonstrated that the intestine is one of the most important target organs for microplastics (Pedà et al., 2016; Lu et al., 2019), but similar studies on octopuses have not been reported previously. There, early inflammatory responses (vacuolation, the shedding of microvilli, and goblet cell increase) were detected in the treatment groups (Jabeen et al., 2018). To resist the impact of microplastics, the first defense strategy with goblet cell increases and looseness of connective tissue in the intestine was activated (Rochman et al., 2014). Subsequently, vacuolation and the shedding of microvilli occur. The severity of damage (significant vacuolation) within the intestine increases with the concentration of exposure (Rochman et al., 2014; Pedà et al., 2016). The release of chemical additives from Micro-PS and the mechanical abrasion may be the main reasons to cause evident morphological abnormalities in intestines (Jabeen et al., 2018; Teng et al., 2021).

4.2. Physiological biomarker responses and integrated biomarker response

A battery of physiological biomarkers was detected to evaluate the toxicity and biological effects of Micro-PS exposure. Firstly, our results

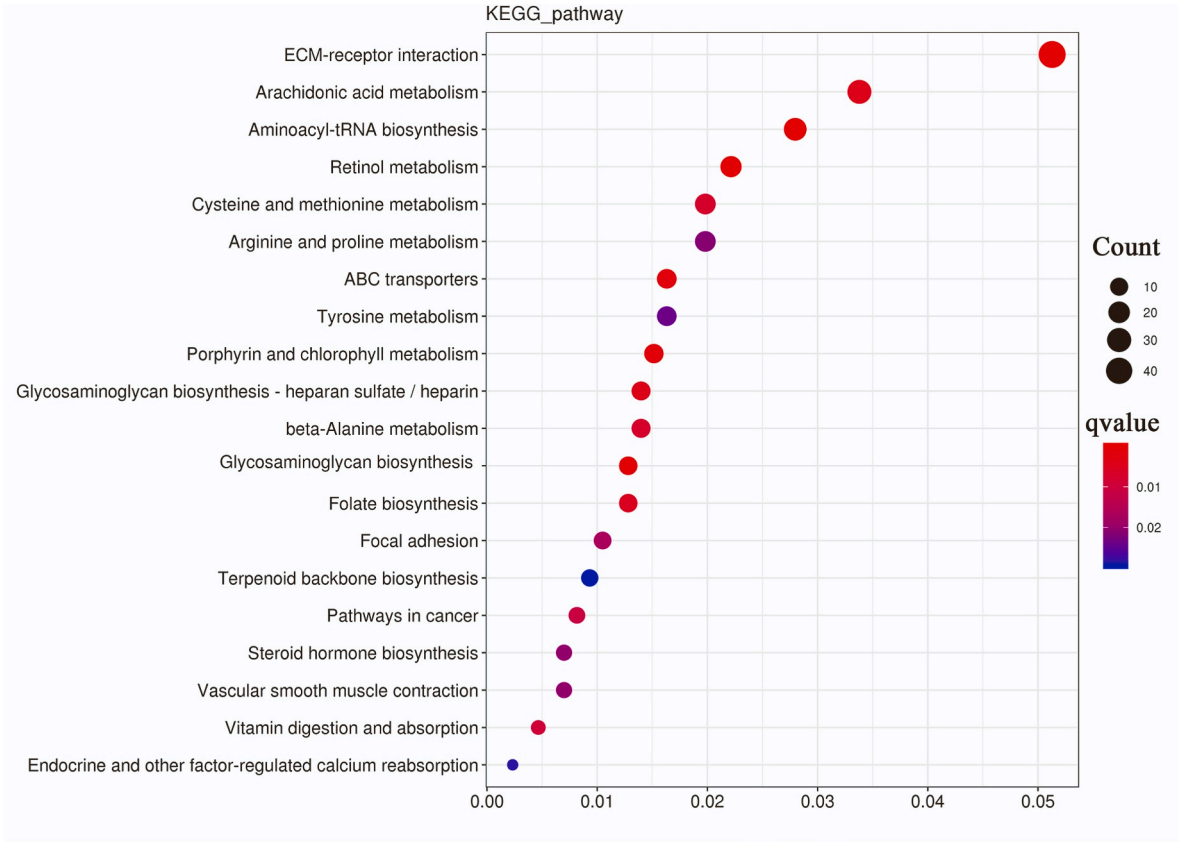

Fig. 7. Several important KEGG pathways that respond to 21-days Micro-PS treatment in *A. fangsiao* (q-value < 0.05).

indicated that oxidative stress response in intestinal cells was exposure concentration-dependent. The Micro-PS can be internalized by the molluscan cells through endocytosis which can lead to oxidative damage. ROS is one of the most commonly used biomarkers to assess the effects of environmental pollution exposure, which is associated with oxidative damage (Avio et al., 2015a). A remarkable increase in intracellular ROS levels was detected in the treatment groups, revealing the strong oxidative damage of Micro-PS exposure in intestinal cells (Paul-Pont et al., 2016). Molluscan cells can counteract the overproduction of ROS by upregulation of the levels and activities of intracellular antioxidants. But this response is limited, which can result in the misbalance between ROS production and antioxidant capacity under high concentrations of Micro-PS exposures (Wang et al., 2018; Huang et al., 2022). In addition, the internalized Micro-PS can interact with other organelles, such as mitochondria, which can also lead to elevated ROS generation (Li et al., 2022). With the accumulation of ROS, MDA content had a considerable improvement after Micro-PS exposure, showing the obvious sign of lipid peroxidation in the intestines. SOD is the main enzyme detoxifying superoxide. It is generated by intracellular and membrane-bound oxidases converting superoxide into freely diffusible hydrogen peroxide (H_2O_2) (Bigorgne et al., 2011). Therefore, the balance of SOD is important for the complete detoxification of superoxide. In this study, due to the high level of oxidative stress, SOD activity was enhanced to cope with the stress in both treatment groups as the intracellular antioxidant enzyme. In addition, CAT is involved in the defense mechanism to resist the exogenous H_2O_2, which plays an important role in removing the main precursor of hydroxyl radical (Avio et al., 2015b). CAT activity was also stimulated in the intestines after Micro-PS exposure, further revealing the apparent antioxidant defense mechanism of *A. fangsiao* to resist Micro-PS toxicity. Overall, our results indicated that Micro-PS exposure can attack the redox system, thus causing the oxidative stress response within intestinal cells.

By contrast, glucose and lipid metabolism markers (Glu, Pyr, T-CHO and TG) have all significantly decreased in the Micro-PS exposure groups. Glucose is broken down into pyruvate in the glycolytic pathway that produces ATP. The decrease of Glu and Pyr indicated that Micro-PS stress induces the disorder of glucose metabolism in the intestine. Similar results were also observed in other marine organisms, such as oysters and zebrafish (Lu et al., 2019; Teng et al., 2021). Besides, lipids in organisms have an important biological function. It is a signaling molecule in cellular regulation and can serve as a structural component of membranes (Filimonova et al., 2016). Lipid changes are usually considered indicators of ecological health and nutritional status in the marine environment (Filimonova et al., 2016). Lipid metabolism is the primary pathway through which energy is supplied to organisms, playing an important role in the response to environmental stress in aquatic invertebrates (Teng et al., 2021). TG and T-CHO are the primary constituents of lipids, which are important energy sources and reserves (Filimonova et al., 2016; Gallardi et al., 2017). They can be hydrolyzed or oxidized to produce energy (Prato et al., 2010; Martínez-Pita et al., 2012). There, we found that the levels of TG and T-CHO in the octopus *A. fangsiao* were reduced with the concentration of Micro-PS. Therefore, our results suggested that Micro-PS exposure is capable of inducing the disorder of glucolipid metabolism.

The IBR approach is a potential ecological risk assessment tool to assess the sensitivity of toxicants in marine organisms (Lin et al., 2014). All physiological biomarkers showed a high response to Micro-PS stress; therefore, they are suitable for IBR index. The varying area of star plots revealed the interactive effect of biomarker responses in intestinal tissues among the groups. IBR values have increased with Micro-PS concentration, suggesting the rising toxic stress in the intestines of *A. fangsiao* (Fig. 3J).

4.3. Microbiome perturbations

Oxidative damage, metabolic disorders and long-term inflammation

in the intestines are inextricably linked with intestinal microbiota dysbiosis (Qiao et al., 2019). In this study, a distinct intestinal microbiota disorder was detected in the PS-H group. This rank abundance curve (Fig. 4D) is designed to measure species richness and evenness in a sample, where a longer curve indicates that there are more species in the sample. It can reflect individual physiological conditions. Our result showed that Micro-PS exposure has reduced intestinal microbial richness and diversity. Previous studies have confirmed microbiota dysbiosis after microplastic exposure, most of which have observed the reduction of intestinal microbiota diversity (Merrifield et al., 2013; Gu et al., 2020). The decline of microbiota diversity may disrupt the stability of the intestinal bacterial community and alter the dominant species of intestinal microbiota, thereby causing inflammatory bowel disease (Riva et al., 2017).

After 21-day Micro-PS exposure, a remarkable change was detected in the diversity and composition of intestinal microflora at the family and genus levels (Fig. 5A and B). The Tenericute generally showed an increasing trend, while Proteobacteria, Spirochaetes and Firmicutes were in a downward trend. There was a close association between the phylum Tenericutes and metabolic health according to previous reports (Lindheim et al., 2017). Lim et al. (2017) detected lower enrichment of Tenericutes in metabolic syndrome patients compare with those in healthy humans. A similar result was also found in *procambarus clarkii* infected with the white spot syndrome virus. Many studies have confirmed Proteobacteria is closely related to the growth of marine organisms (Roh and Seki, 2013; Li et al., 2017). The reduction of Proteobacteria observed in this study may stunt the growth of *A. fangsiao*. Moreover, the low abundance of Spirochaetes and Firmicutes was also detected, indicating that *A. fangsiao* under Micro-PS exposure has a lower effect to get energy from food (Ley et al., 2006; Gu et al., 2020). Likewise, the disorder of intestinal microflora at the genus level was detected in the treatment group. Overall, Micro-PS exposure has changed the composition and diversity of intestinal microflora, thereby harmful to the intestinal health of *A. fangsiao*.

4.4. Transcriptomic responses

Transcriptomic analysis plays an important role in studying cell phenotype and function, which can reflect the tissue damage at the molecular level. The histological damage, oxidative damage, and glucolipid metabolism disorders in intestines have been detected based on the above studies. Related DEGs and significantly enriched pathways were also found in transcriptome analysis, further confirming these results.

The downregulation of several rate-limiting enzyme genes in glycolytic pathway (phosphoenolpyruvate carboxykinase 1, *PEPckc* and pyruvate kinase, *PK*) was detected based on transcriptomic analysis and qRT-PCR experiment (Fig. 8, Fig. S3) (Wright et al., 2013; Méndez-Lucas et al., 2014). Microplastics can block enzyme production, thereby causing metabolism disorders in aquatic animals (Zhao et al., 2020). Peroxisome proliferators-activated receptors (PPARs) family involved in the regulation of lipogenesis, which has been confirmed in many studies (Browning and Horton, 2004; Zhao et al., 2020). Therefore, the downregulation of *PPAR-α* gene detected in this study supported the disorder of lipid metabolism in the intestinal cells of *A. fangsiao* (Nguyen et al., 2008). In addition, terpenoid backbone biosynthesis and steroid hormone biosynthesis in response to metabolism were significantly enriched in this study, revealing the strong impact of Micro-PS exposure on metabolism of *A. fangsiao* (Zhao et al., 2020).

The pathway of arachidonic acid metabolism, arginine and proline metabolism were significantly enriched after 21-day Micro-PS exposure, resulting from the high content of ROS (Fig. 8). In the pathway of arachidonic acid metabolism, the arachidonic acid metabolite is oxidized by prostaglandin H synthase and lipoxygenases where ROS are generated as byproducts (Kim and Kim, 2008; Dohnal et al., 2014). As the important components of arginine and proline metabolism pathway, proline, ornithine and glutamine were involved profoundly in the proline-dependent production of ROS related to the cellular redox reactions (Lu et al., 2019). Besides, our transcriptomic and qRT-PCR analyses indicated that *aquaporin* and *ferritin* genes were significantly up-regulated and down-regulated, respectively, both of which participate in the progress of oxidative stress (Park and Chung, 2019; Knaus, 2020).

Many studies have demonstrated that microplastics can interact with the surface receptors on the membrane as well as penetrate the lipid bilayer inducing structural changes to the membrane (Holloczki and Gehrke, 2020; Li et al., 2022). Our study detected that Micro-PS

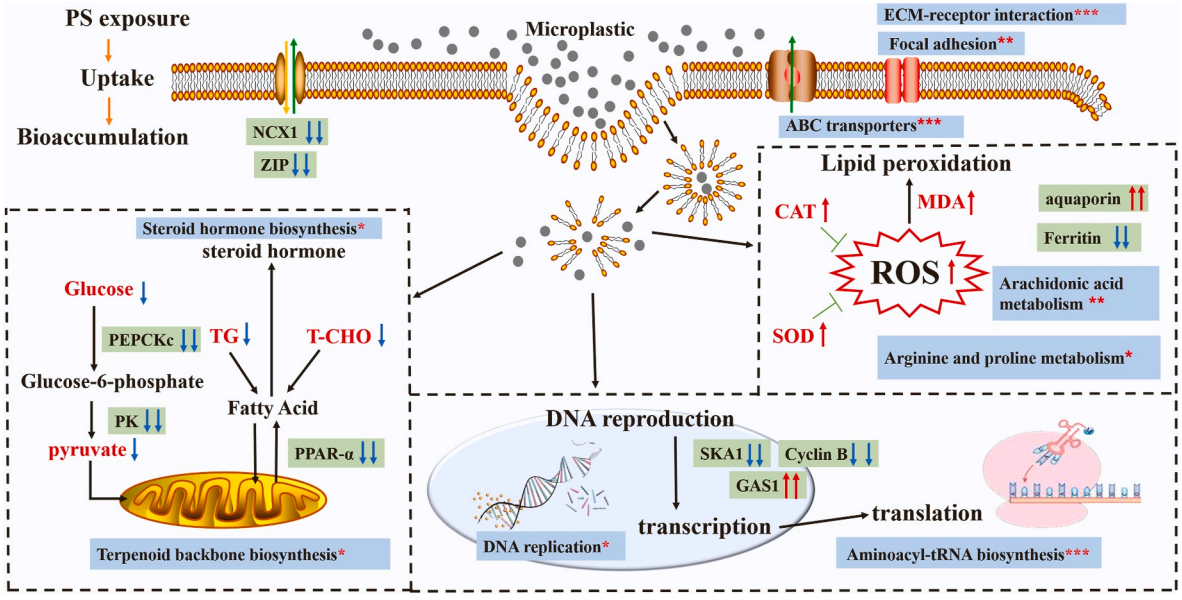

Fig. 8. Schematic representation of biological pathways in *A. fangsiao* affected by Micro-PS. The green box represents the gene; the blue box represents the KEGG pathway. The red font represents biomarkers. Asterisks indicate significantly enriched pathways (***q-value < 0.001, ** q-value < 0.01, * q-value < 0.05). The two arrows in the green box represent the regulation of genes based on transcriptomic and qRT-PCR analysis. Other arrows represent the regulation of biomarkers. (For interpretation of the references to color in this figure legend, the reader is referred to the Web version of this article.)

exposure has an impact on the transmembrane transport of intestinal cells, which supported this conclusion. The pathway of ATP-binding cassette (ABC) transporters catalyzed transport reactions were significantly enriched based on KEGG enrichment analysis (Fig. 8). ECM-receptor interaction pathways and focal adhesion can lead to direct or indirect control of cellular activities such as adhesion, migration, differentiation, proliferation, and apoptosis. The significant enrichment of these pathways indicated that exposure to microplastics caused a huge influence on the maintenance of cell and tissue structure and function. Moreover, several DEGs (sodium/calcium exchanger, *NCX* and zinc transporters, *ZIP*) associated with transmembrane transport also exhibited a markable down-regulation. As a plasma membrane resident protein, sodium-/calcium exchanger is related to the bidirectional transport of Ca^{2+} and Na^{+}. It can exchange Ca^{2+} from one side of the membrane with Na^{+} on the other side. The down-regulation of *NCX* gene resulted in the imbalance of Na^{+} and Ca^{2+} transmembrane transport. Similarly, the imbalance of Zn^{2+} transmembrane transport was also confirmed by the down-regulation of *ZIP* gene.

Previous studies have reported microplastic exposure can cause DNA damage to marine organisms (Roda et al., 2020; Alnajar et al., 2021), which was also confirmed in the present study. KEGG enrichment analysis indicated that several pathways exhibited remarkable enrichment in DNA damage and translation progress, including DNA replication and AminoacyI-tRNA biosynthesis. Moreover, several down-regulated genes (*SKA1* and *GAS1*) related to DNA damage were detected after 21-day Micro-PS exposure. Cell cycle arrest is usually associated with DNA damage (Eom and Choi, 2010). Pan et al. (2018) reported that 12-h AgNPs exposure has led to the upregulation of G1/S specific cyclin E (CycE) gene whose encoded protein controls G1 to S transition. In our study, gene G2/mitotic specific cyclin B (CycB) which controls the G2 to M progression downregulated in Control vs. PS-H groups (Fig. 8), indicating that Micro-PS might lead to G2/M arrest, thereby causing apoptosis. These results showed that a high concentration of Micro-PS exposure might have caused DNA damage and triggered a response to repair the damage via transcriptional and post-transcriptional regulation.

5. Conclusion

In summary, this study highlights the responses of physiology, microbiome and transcriptome in the intestine of *A. fangsiao* under Micro-PS exposure stress, which provides insights into the mechanisms of damage at different biological levels. Significant damage was detected from physiological responses to molecular mechanisms, as our data suggest. Micro-PS exposure can lower food intake, and promote histopathological alterations. Oxidative stress and metabolism disorders were further generated. It also indicated that Micro-PS exposure altered the transcriptomic profiles, including transmembrane transport of intestinal cells and DNA damage. These results provide basic data for risk assessment of Micro-PS exposure on the octopus. Recommendations for future microplastic exposure experiments are studies based on diverse types, shapes and sizes of microplastics with environmentally relevant properties.

Funding

We acknowledge grant support from the National Natural Science Foundation of China (32170536) and the National Key Research and Development Program of China (2020YFD0900705).

Author contributions

Jian Zheng and Xiaodong Zheng conceived and designed the experiments; Jian Zheng and Congjun Li performed the experiments; Jian Zheng analyzed the data; Jian Zheng and Xiaodong Zheng contributed materials tools; Jian Zheng and Congjun Li wrote the manuscript, and Xiaodong Zheng reviewed the manuscript.

Declaration of competing interest

The authors declare that they have no known competing financial interests or personal relationships that could have appeared to influence the work reported in this paper.

Data availability

Data will be made available on request.

Appendix A. Supplementary data

Supplementary data to this article can be found online at https://doi.org/10.1016/j.chemosphere.2022.136362.

References

Alnajar, N., Jha, A.N., Turner, A., 2021. Impacts of microplastic fibres on the marine mussel, *Mytilus galloprovinciallis*. Chemosphere 262, 128290.
Anderson, M.J., 2005. PERMANOVA: a FORTRAN Computer Program for Permutational Multivariate Analysis of Variance.
Angiolillo, M., Fortibuoni, T., 2020. Impacts of marine litter on Mediterranean reef systems: from shallow to deep waters. Front. Mar. Sci. 7, 826.
Angiolillo, M., G'erigny, O., Valente, T., Fabri, M.-C., Tambute, E., Rouanet, E., Claro, F., Tunesi, L., Vissio, A., Daniel, B., 2021. Distribution of seafloor litter and its interaction with benthic organisms in deep waters of the Ligurian Sea (Northwestern Mediterranean). Sci. Total Environ. 788, 147745.
Arechavala-Lopez, P., Minguito-Frutos, M., Follana-Berná, G., Palmer, M., 2018. Common octopus settled in human-altered mediterranean coastal waters: from individual home range to population dynamics. ICES J. Mar. Sci. 2, 2.
Avio, C.G., Gorbi, S., Milan, M., Benedetti, M., Fattorini, D., d Errico, G., Pauletto, M., Bargelloni, L., Regoli, F., 2015a. Pollutants bioavailability and toxicological risk from microplastics to marine mussels. Environ. Pollut. 198, 211e222.
Avio, C.G., Gorbi, S., Regoli, F., 2015b. Experimental development of a new protocol for extraction and characterization of microplastics in fish tissues: first observations in commercial species from Adriatic Sea. Mar. Environ. Res. 111, 18e26.
Bao, X.K., Wang, W.J., Yuan, T.Z., Li, Y., Chen, X.P., Liu, X.M., Xu, X.H., Sun, G.H., Li, B., Yang, J.M., Feng, Y.W., Li, Z., 2022. Transcriptome profiling based on larvae at different time points after hatching provides a core set of gene resource for understanding the immune response mechanisms of the egg-protecting behavior against *Vibrio anguillarum* infection in *Amphioctopus fangsiao*. Fish Shellfish Immunol. 124, 430–441.
Beiras, R., Schönemann, A.M., 2020. Currently monitored microplastics pose negligible ecological risk to the global ocean. Sci. Rep. 10 (1), 1–9.
Beliaeff, B., Burgeot, T., 2002. Integrated biomarker response: a useful tool for ecological risk assessment. Environ. Toxicol. Chem. 21 (6), 1316–1322.
Bidder, A.M., 1966. Feeding and digestion in cephalopods. In: Wilber, K.M., Yonge, C.M. (Eds.), Physiology of the Mollusca Vol. II. Academic Press, N. Y., pp. 97–124
Biginagwa, F.J., Maymoa, B.S., Shashoua, Y., Syberg, K., Khan, F.R., 2016. First evidence of microplastics in the african great lakes: recovery from lake victoria nile perch and nile tilapia. J. Gt. Lakes Res. 42, 146e149.
Bigorgne, E., Foucaud, L., Lapied, E., Labile, J., Botta, C., Sirguey, C., 2011. Ecotoxicological assessment of TiO_2 byproducts on the earthworm *Eisenia fetida*. Environ. Pollut. 159, 2698–2705.
Bo, Q.K., Zheng, X.D., Chen, Z.W., 2020. Feeding intensity and molecular prey identification of the common long-armed octopus *Octopus minor*, (mollusca: octopodidae) in the wild. PLoS One 15 (1), e0220482.
Bolger, A.M., Lohse, M., Usadel, B., 2014. Trimmomatic: a flexible trimmer for Illumina sequence data. Bioinformatics 30 (15), 2114–2120.
Browning, J.D., Horton, J.D., 2004. Molecular mediators of hepatic steatosis and liver injury. Clin. Invest. 114, 147–152.
Caporaso, J.G., Kuczynski, J., Stombaugh, J., Bittinger, K., Bushman, F.D., Costello, E.K., Fierer, N., Peña, A.G., Goodrich, J.K., Gordon, J.I., Huttley, G.A., Kelley, S.T., Knights, D., Koenig, J.E., Ley, R.E., Lozupone, C.A., McDonald, D., Muegge, B.D., Pirrung, M., Reeder, J., Sevinsky, J.R., Turnbaugh, P.J., Walters, W.A., Widmann, J., Yatsunenko, T., Zaneveld, J., Knight, R., 2010. QIIME allows analysis of high-throughput community sequencing data. Nat. Methods 7 (5), 335–336.
Consoli, P., Romeo, T., Angiolillo, M., Canese, S., Esposito, V., Salvati, E., Scotti, G., Andaloro, F., Tunesi, L., 2019. Marine litter from fishery activities in the Western Mediterranean Sea: the impact of entanglement on marine animal forests. Environ. Pollut. 249, 472–481.
Dohnal, V., Wu, Q., Kuca, K., 2014. Metabolism of aflatoxins: key enzymes and interindividual as well as interspecies differences. Arch. Toxicol. 88, 1635–1644.
Dong, M., Zhu, L., Zhu, S., Wang, J., Wang, J., Xie, H., Du, Z., 2013. Toxic effects of 1-decyl-3-methylimidazolium bromide ionic liquid on the antioxidant enzyme system and DNA in zebrafish (*Danio rerio*) livers. Chemosphere 91 (8), 1107–1112.
Dou, P.C., Mai, L., Bao, L.J., Zeng, E.Y., 2021. Microplastics on beaches and mangrove sediments along the coast of South China. Mar. Pollut. Bull. 172, 112806.

Edgar, R.C., 2013. UPARSE: highly accurate OTU sequences from microbial amplicon reads. Nat. Methods 10 (10), 996.
Eo, S., Hong, S.H., Song, Y.K., Lee, J., Lee, J., Shim, W.J., 2018. Abundance, composition, and distribution of microplastics larger than 20 μm in sand beaches of South Korea. Environ. Pollut. 238, 894–902.
Eom, H.J., Choi, J., 2010. p38 MAPK activation, DNA damage, cell cycle arrest and apoptosis as mechanisms of toxicity of silver nanoparticles in Jurkat T cells. Environ. Sci. Technol. 44 (21), 8337–8342.
Eriksen, M., Lebreton, L., Carson, H.S., Thiel, M., Reisser, J., 2014. Plastic pollution in the world's oceans: more than 5 trillion plastic pieces weighing over 250,000 tons afloat at sea. PLoS One 9 (12), e111913.
Ferreira, G.V.B., Justino, A.K.S., Eduardo, L.N., Lenoble, V., Fauvelle, V., Schmidt, N., Junior, T.V., Frédou, T., Lucena-Frédou, F., 2022. Plastic in the inferno: microplastic contamination in deep-sea cephalopods (*Vampyroteuthis infernalis* and *Abralia veranyi*) from the southwestern Atlantic. Mar. Pollut. Bull. 174, 113309.
Filimonova, V., Goncalves, F., Marques, J.C., De Troch, M., Goncalves, A.M., 2016. Biochemical and toxicological effects of organic (herbicide Primextra Gold TZ) and inorganic (copper) compounds on zooplankton and phytoplankton species. Aquat. Toxicol. 177, 33e43.
Galgani, F., Hanke, G., Maes, T., 2015. Global distribution, composition and abundance of marine litter. In: Marine Anthropogenic Litter. Springer, Cham, pp. 29–56.
Gallardi, D., Mills, T., Donnet, S., Parrish, C.C., Murray, H.M., 2017. Condition and biochemical profile of blue mussels (*Mytilus edulis L.*) cultured at different depths in a cold water coastal environment. J. Sea Res. 126, 37e45.
Garces-Ordonez, O., Espinosa, L.F., Cardoso, R.P., Cardozo, B.B.I., dos Anjos, R.M., 2020. Plastic litter pollution along sandy beaches in the Caribbean and Pacific coast of Colombia. Environ. Pollut. 267, 115495.
García, B.G., Giménez, F.A., 2002. Influence of diet on growing and nutrient utilization in the common octopus (*Octopus vulgaris*). Aquaculture 211, 171–182.
Gong, Y., Wang, Y., Chen, L., Li, Y., Liu, B., 2021. Microplastics in different tissues of a pelagic squid (*Dosidicus gigas*) in the northern Humboldt current ecosystem. Mar. Pollut. Bull. 169, 112509.
Gower, J.C., 1966. Some distance properties of latent root and vector methods used in multivariate analysis. Biometrika 53 (3–4), 325–338.
Green, D.S., 2016. Effects of microplastics on European flat oysters, Ostrea edulis and their associated benthic communities. Environ. Pollut. 216, 95–103, 2016.
Gu, H., Wang, S., Wang, X., Yu, X., Hu, M., Huang, W., Wang, Y., 2020. Nanoplastics impair the intestinal health of the juvenile large yellow croaker *Larimichthys crocea*. J. Hazard Mater. 5 (397), 122773.
Hanbo, C., Paul, C.B., 2011. VennDiagram: a package for the generation of highly-customizable Venn and Euler diagrams in R. BMC Bioinf. 12 (1), 35.
Hirt, N., Body-Malapel, M., 2020. Immunotoxicity and intestinal effects of nano- and microplastics: a review of the literature. Part. Fibre Toxicol. 17 (1), 57.
Holloczki, O., Gehrke, S., 2020. Can nanoplastics alter cell membranes? ChemPhysChem 21 (1), 9.
Hsu, C.Y., Chiu, Y.C., Hsu, W.L., Chan, Y.P., 2008. Age-related markers assayed at different developmental stages of the annual fish *Nothobranchius rachovii*. J Gerontol A Biol Sci Med Sci 63 (12), 1267–1276.
Hua, G.J., Hung, C.L., Lin, C.Y., Wu, F.C., Chan, Y.W., Tang, C.Y., 2017. MGUPGMA: a fast UPGMA algorithm with multiple graphics processing units using nccl. Evol. Bioinf. Online 13, 1176934317734220.
Huang, W., Wang, X.H., Chen, D.Y., Xu, E.G., Luo, X., Zeng, J.N., Huan, T., Li, L., Wang, Y.J., 2021. Toxicity mechanisms of polystyrene microplastics in marine mussels revealed by high-coverage quantitative metabolomics using chemical isotope labeling liquid chromatography mass spectrometry. J. Hazard Mater. 417, 126003.
Huang, X.Z., Leung, J., Hu, M.H., Xu, E.G., Wang, Y.J., 2022. Microplastics can aggravate the impact of ocean acidification on the health of mussels: insights from physiological performance, immunity and byssus properties. Environ. Pollut. 308, 119701.
Jabeen, K., Li, B., Chen, Q., Su, L., Wu, C., Hollert, H., Shi, H., 2018. Effects of virgin microplastics on goldfish (*Carassius auratus*). Chemosphere 213, 323–332.
Jiang, D.H., Zheng, X.D., Qian, Y.S., Zhang, Q.Q., 2020a. Embryonic development of *amphioctopus fangsiao* under elevated temperatures: implications for resource management and conservation. Fish. Res. 225, 105479.
Jiang, D.H., Zheng, X.D., Qian, Y.S., Zhang, Q.Q., 2020b. Development of *Amphioctopus fangsiao* (Mollusca: cephalopoda) from eggs to hatchlings: indications for the embryonic developmental management. Mar. Life. Sci. Tech. 2 (1), 7.
Jin, Y.X., Xia, J.H., Pan, Z.H., Yang, J.J., Wang, W.W., 2018. Polystyrene microplastics induce microbiota dysbiosis and inflammation in the gut of adult zebrafish. Environ. Pollut. 235, 322-329.
Kim, C.M., Kim, J.H., 2008. BMB reports: mini review; cytosolic phospholipase A2, lipoxygenase metabolites, and reactive oxygen species. Biochem. Mol. Biol. Rep. 41, 555–559.
Kim, D., Langmead, B., Salzberg, S.L., 2015. HISAT: a fast spliced aligner with low memory requirements. Nat. met. 12 (4), 357–360.
Knaus, U.G., 2020. Oxidants in physiological processes. Handb. Exp. Pharmacol. 264, 27–47.
Kõljalg, U., Nilsson, R.H., Abarenkov, K., Tedersoo, L., Taylor, A.F., Bahram, M., Bates, S. T., Bruns, T.D., Bengtsson-Palme, J., Callaghan, T.M., Douglas, B., Drenkhan, T., Eberhardt, U., Dueñas, M., Grebenc, T., Griffith, G.W., Hartmann, M., Kirk, P.M., Kohout, P., Larsson, E., Larsson, K.H., 2013. Towards a unified paradigm for sequence-based identification of fungi. Mol. Ecol. 22 (21), 5271–5277.
Kuhn, S., van Franeker, J.A., 2020. Quantitative overview of marine debris ingested by marine megafauna. Mar. Pollut. Bull. 151, 110858.
Kühn, S., Rebolledo, E.L.B., Van Franeker, J.A., 2015. Deleterious effects of litter on marine life. Mar. Anthropog. Litter. 6, 75–116.
Ley, R.E., Turnbaugh, P.J., Klein, S., Gordon, J.I., 2006. Microbial ecology-Human gut microbes associated with obesity. Nature 444, 1022–1023.
Li, Y.Y., Chen, X., Song, T.Y., 2017. Differences in intestinal flora of cultured large yellow croaker *Pseudosciaena crocea* with different growth rates. Journal of Dalian Ocean University 32 (5), 509–513 (in Chinese).
Li, Z.Q., Chang, X.Q., Hu, M.H., Fang, J.K., Sokolova, I.M., Huang, W.H., Xu, E.G., Wang, Y.J., 2022. Is microplastic an oxidative stressor? Evidence from a meta-analysis on bivalves. J. Hazard Mater. 423 (Pt B), 127211.
Lim, M.Y., You, H.J., Yoon, H.S., Kwon, B., Lee, J.Y., Lee, S., Song, Y.M., Lee, K., Sung, J., Ko, G., 2017. The effect of heritability and host genetics on the gut microbiota and metabolic syndrome. Gut 66 (6), 1031–1038.
Lin, T., Yu, S., Chen, Y., Chen, W., 2014. Integrated biomarker responses in zebrafish exposed to sulfonamides. Environ. Toxicol. Pharmacol. 38 (2), 444–452.
Lindheim, L., Bashir, M., Münzker, J., Trummer, C., Zachhuber, V., Leber, B., Horvath, A., Pieber, T.R., Gorkiewicz, G., Stadlbauer, V., Obermayer-Pietsch, B., 2017. Alterations in gut microbiome composition and barrier function are associated with reproductive and metabolic defects in women with polycystic ovary syndrome (PCOS): a pilot study. PLoS One 12 (1), e0168390.
Lipiński, M.R., 1990. Changes in pH in the caecum of *Loligo vulgaris reynaudii* during digestion. S. Afr. J. Mar. Sci. 9, 43–51.
Liu, Z., Yu, P., Cai, M., Wu, D., Zhang, M., Huang, Y., Zhao, Y., 2019. Polystyrene nanoplastic exposure induces immobilization, reproduction, and stress defense in the freshwater cladoceran Daphnia pulex. Chemosphere 215, 74–81.
Love, M.I., Huber, W., Anders, S., 2014. Moderated estimation of fold change and dispersion for RNA-seq data with DESeq2. Genome Biol. 15, 550.
Lu, F., Liu, Y., Guo, Y., Gao, Y., Piao, Y., Tan, S., Tang, Y., 2019. Metabolomic changes of blood plasma associated with two phases of rat OIR. Exp. Eye Res. 190, 107855.
Lucia, M., André, J.M., Gonzalez, P., Baudrimont, M., Bernadet, M.D., Gontier, K., Maury Brachet, R., Guy, G., Davail, S., 2010. Effect of dietary cadmium on lipid metabolism and storage of aquatic bird Cairina moschata. Ecotoxicology 19, 163.
Lusher, A., 2015. Microplastics in the marine environment: distribution, interactions and effects. In: Bergmann, M.E.A. (Ed.), Marine Anthropogenic Litter. Springer International Publishing, Switzerland, pp. 245–307.
Mangold, K., 1983. Octopus vulgaris. In: Boyle, P. (Ed.), Cephalopod Life Cycles, Species Accounts, vol. I. Academic Press, United Kingdom, p. 335e364.
Martin, M., 2011. Cutadapt removes adapter sequences from high-throughput sequencing reads. Embnet. J. 17 (1).
Martínez-Pita, I., Smanchez-Lazo, C., Ruíz-Jarabo, I., Herrera, M., Mancera, J.M., 2012. Biochemical composition, lipid classes, fatty acids and sexual hormones in the mussel *Mytilus galloprovincialis* from cultivated populations in south Spain. Aquaculture 358, 274e283.
Méndez-Lucas, A., Hyroššová, P., Novellasdemunt, L., Viñals, F., Perales, J.C., 2014. Mitochondrial phosphoenolpyruvate carboxykinase (PEPCK-M) is a pro-survival, endoplasmic reticulum (ER) stress response gene involved in tumor cell adaptation to nutrient availability. J. Biol. Chem. 289 (32), 22090–22102.
Merrifield, D.L., Shaw, B.J., Harper, G.M., Saoud, I.P., Davies, S.J., Handy, R.D., Henry, T.B., 2013. Ingestion of metal-nanoparticle contaminated food disrupts endogenous microbiota in zebrafish (*Danio rerio*). Environ. Pollut. 174, 157–163.
Nelms, S.E., Galloway, T.S., Godley, B.J., Jarvis, D.S., Lindeque, P.K., 2018. Investigating microplastic trophic transfer in marine top predators. Environ. Pollut. 238, 999–1007.
Nguyen, P., Leray, V., Diez, M., Serisier, S., Le Bloc'h, J., Siliart, B., 2008. Liver lipid metabolism. J. Anim. Physiol. Anim. Nutr. 92, 272–283.
Okutan, H., Ozcelik, N., Yilmaz, H.R., Uz, E., 2005. Effects of caffeic acid phenethyl ester on lipid peroxidation and antioxidant enzymes in diabetic rat heart. Clin. Biochem. 38 (2), 191–196.
Oliveira, A.R., Sardinha-Silva, A., Andrews, P.L.R., Green, D., Cooke, G.M., Hall, S., Blackburn, K., Sykes, A.V., 2020. Microplastics presence in cultured and wild-caught cuttlefish, Sepia officinalis. Mar. Pollut. Bull. 160, 111553.
Ory, N.C., Gallardo, C., Lenz, M., 2018. Capture, swallowing, and egestion of microplastics by a planktivorous juvenile fish. Environ. Pollut. 240, 566–573.
Pan, Y.B., Zhang, W.J., Lin, S.J., 2018. Transcriptomic and microRNAomic profiling reveals molecular mechanisms to cope with silver nanoparticle exposure in the ciliate *Euplotes vannus*. Environ. Sci. Nano. 5 (12), 2921–2935.
Park, E., Chung, S.W., 2019. ROS-mediated autophagy increases intracellular iron levels and ferroptosis by ferritin and transferrin receptor regulation. Cell Death Dis. 10 (11), 822.
Paul-Pont, I., Lacroix, C., González, Fernández, C., Hégaret, H., Lambert, C., Le Goïc, N., Frère, L., Cassone, A.L., Sussarellu, R., Fabioux, C., Guyomarch, J., Albentosa, M., Huvet, A., Soudant, P., 2016. Exposure of marine mussels Mytilus spp. to polystyrene microplastics: toxicity and influence on fluoranthene bioaccumulation. Environ. Pollut. 216, 724–737.
Pedà, Caccamo, Fossi, M.C., Gai, F., Andaloro, F., Genovese, L., Perdichizzi, A., Romeo, T., Maricchiolo, G., 2016. Intestinal alterations in European sea bass Dicentrarchus labrax (Linnaeus, 1758) exposed to microplastics: preliminary results. Environ. Pollut. 212, 251–256.
Pedà, C., Longo, F., Berti, C., Laface, F., De Domenico, F., Consoli, P., Battaglia, P., Greco, S., Romeo, T., 2022. The waste collector: information from a pilot study on the interaction between the common octopus (*Octopus vulgaris*, Cuvier, 1797) and marine litter in bottom traps fishing and first evidence of plastic ingestion. Mar. Pollut. Bull. 174, 113185.
Pertea, M., Pertea, G.M., Antonescu, C.M., Chang, T.C., Mendell, J.T., Salzberg, S.L., 2015. StringTie enables improved reconstruction of a transcriptome from RNA-seq reads[J]. Nat. Biotechnol. 33 (3), 290–295.

Pham, C.K., Ramirez-Llodra, E., Alt, C.H.S., Amaro, T., Bergmann, M., Canals, M., Davies, J., Duineveld, G., Galgani, F., Howell, K.L., 2014. Marine litter distribution and density in European seas, from the shelves to deep basins. PLoS One 9, e95839.
Prato, E., Danieli, A., Maffia, M., Biandolino, F., 2010. Lipid and fatty acid compositions of *Mytilus galloprovincialis* cultured in the mar grande of taranto (southern Italy): feeding strategies and trophic relationships. Zool. Stud. 49 (2), 211–219.
Qiao, R., Sheng, C., Lu, Y., Zhang, Y., Ren, H., Lemos, B., 2019. Microplastics induce intestinal inflammation, oxidative stress, and disorders of metabolome and microbiome in zebrafish. Sci. Total Environ. 662, 246–253.
Raimundo, J., Vale, C., Canário, J., Branco, V., Moura, I., 2010. Relations between mercury, methyl-mercury and selenium in tissues of *Octopus vulgaris* from the Portuguese coast. Environ. Pollut. 158 (6), 2094–2100.
Riva, A., Borgo, F., Lassandro, C., Verduci, E., Morace, G., Borghi, E., Berry, D., 2017. Pediatric obesity is associated with an altered gut microbiota and discordant shifts in Firmicutes populations. Environ. Microbiol. 19, 95–105.
Rochman, C.M., Kurobe, T., Flores, I., The, S.J., 2014. Early warning signs of endocrine disruption in adult fish from the ingestion of polyethylene with and without sorbed chemical pollutants from the marine environment. Sci. Total Environ. 493, 656–661.
Roda, J.F.B., Lauer, M.M., Risso, W.E., Bueno, Dos, R., Martinez, C., 2020. Microplastics and copper effects on the neotropical teleost *Prochilodus lineatus*: is there any interaction? Comp. Biochem. Physiol. A. Mol. Integr. Physiol. 242, 110659.
Roh, Y.S., Seki, E., 2013. Toll-like receptors in alcoholic liver disease, non-alcoholic steatohepatitis and carcinogenesis. J. Gastroenterol. Hepatol. 28 (Suppl. 1), 38–42.
Samanta, P., Im, H., Na, J., Jung, J., 2018. Ecological risk assessment of a contaminated stream using multi-level integrated biomarker response in *Carassius auratus*. Environ. Pollut. 233, 429e438.
Sanchez, W., Bender, C., Porcher, J.M., 2014. Wild gudgeons (*Gobio gobio*) from French rivers are contaminated by microplastics: preliminary study and first evidence. Environ. Res. 128, 98–100.
Sanchez, W., Burgeot, T., Porcher, J.M., 2013. A novel 'integrated biomarker response' calculation based on reference deviation concept. Environ. Sci. Pollut. Res. 20 (5), 2721–2725.
Semedo, M., Valentim, D., Gomes, F., Oliveira, M., Delerue-Matos, C., Henriques, M.A., 2014. Common octopus (*Octopus vulgaris*), as a New Bioindicator Species for Coastal Pollution Monitoring, pp. 14–16.
Sillero-Ríos, J., Sureda, A., Capó, X., Oliver-Codorniú, M., Arechavala-Lopez, P., 2018. Biomarkers of physiological responses of *Octopus vulgaris* to different coastal environments in the western Mediterranean Sea. Mar. Pollut. Bull. 128, 240–247.
Song, M.P., Wamg, J.H., Chen, Z.W., Li, X.B., Zheng, X.D., 2020. Effects of starvation on survival, growth and muscle fatty acids, amino acids of *Octopus minor*. Acta Hydrobiol. Sin. 2020 (2), 372–378 (In Chinese).
Spitz, D.R., Oberley, L.W., 1989. An assay for superoxide dismutase activity in mammalian tissue homogenates. Anal. Biochem. 179 (1), 8–18.
Sussarellu, R., Suquet, M., Thomas, Y., Lambert, C., Fabioux, C., Pernet, M.E.J., Goïc, N. L., Quillien, V., Mingant, C., Epelboin, Y., Corporeau, C., Guyomarch, J., Robbens, J., Paul-Pont, I., Soudant, P., Huvet, A., 2016. Oyster reproduction is affected by exposure to polystyrene microplastics. P. Natl. Acad. Sci. 113 (9), 2430e2435. https://doi.org/10.1073/pnas.1519019113.
Tang, Y., Zhang, X.Y., Ma, Y., Zheng, X.D., 2021. Descriptive study of the mitogenome of the diamondback squid (*Thysanoteuthis rhombus troschel*, 1857) and the evolution of mitogenome arrangement in oceanic squids. J. Zool. Syst. Evol. Res. 1–11, 00.
Teng, J., Zhao, J., Zhu, X., Shan, E., Zhang, C., Zhang, W., Wang, Q., 2021. Toxic effects of exposure to microplastics with environmentally relevant shapes and concentrations: accumulation, energy metabolism and tissue damage in oyster Crassostrea gigas. Environ. Pollut. 269, 116169.
Thiel, M., Hinojosa, I.A., Miranda, L., Pantoja, J.F., Rivadeneira, M.M., Vasquez, N., 2013. Anthropogenic marine debris in the coastal environment: a multi-year comparison between coastal waters and local shores. Mar. Pollut. Bull. 71, 307–316.
Wang, F., Salvati, A., Boya, P., 2018. Lysosome-dependent cell death and deregulated autophagy induced by amine-modified polystyrene nanoparticles. Open Biol 8 (4), 170271.
Wang, S.X., Zhong, Z., Li, Z.Q., Wang, X.H., Gu, H.X., Huang, W., Fang, J.K., Shi, H.H., Hu, M.H., Wang, Y.J., 2021. Physiological effects of plastic particles on mussels are mediated by food presence. J J. Hazard. Mater. 404 (Pt A), 124136.
Weber, A., Jeckel, N., Wagner, M., 2020. Combined effects of polystyrene microplastics and thermal stress on the freshwater mussel Dreissena polymorpha. Sci. Total Environ. 718, 137253 https://doi.org/10.1016/j.scitotenv.2020.137253.
Wegner, A., Besseling, E., Foekema, E.M., Kamermans, P., Koelmans, A.A., 2012. Effects of nanopolystyrene on the feeding behavior of the blue mussel (Mytilus edulis L.). Environ. Toxicol. Chem. 31 (11), 2490–2497. https://doi.org/10.1002/etc.1984.
Wright, S.L., Thompson, R.C., Galloway, T.S., 2013. The physical impacts of microplastics on marine organisms: a review. Environ. Pollut. 178, 483–492.
Xu, X.Y., Lee, W.T., Chan, A.K.Y., Lo, H.S., Shin, P.K.S., Cheung, S.G., 2017. Microplastic ingestion reduces energy intake in the clam Atactodea striata. Mar. Pollut. Bull. 124 (2), 798–802. https://doi.org/10.1016/j.marpolbul.2016.12.027.
Zhao, Y., Bao, Z., Wan, Z., Fu, Z., Jin, Y., 2020. Polystyrene microplastic exposure disturbs hepatic glycolipid metabolism at the physiological, biochemical, and transcriptomic levels in adult zebrafish. Sci. Total Environ. 710, 136279.
Zielinski, S., Pörtner, H.O., 2000. Oxidative stress and antioxidative defense in cephalopods: a function of metabolic rate or age? Comp. Biochem. Physiol. B Biochem. Mol. Biol. 125 (2), 147–160.
Zuo, L., Sun, Y., Li, H., Hu, Y., Lin, L., Peng, J., Xu, X., 2020. Microplastics in mangrove sediments of the Pearl River estuary, South China: correlation with halogenated flame retardantsapos; levels. Sci. Total Environ. 725, 138344.